DEUTSCHES ELEKTRONEN – SYNCHROTRON

DESY 92-117
August 1992

On the Kinetics of the Electroweak Phase Transition

W. Buchmüller, T. Helbig

Deutsches Elektronen-Synchrotron DESY, Hamburg

ISSN 0418-9833

NOTKESTRASSE 85 · D-2000 HAMBURG 52

To be sure that your preprints are promptly included in the
HIGH ENERGY PHYSICS INDEX,
send them to (if possible by air mail):

DESY
Bibliothek
Notkestraße 85
W-2000 Hamburg 52
Germany

DESY-IfH
Bibliothek
Platanenallee 6
O-1615 Zeuthen
Germany

DESY 92-117
August 1992

ISSN 0418-9833

ON THE KINETICS OF THE ELECTROWEAK PHASE TRANSITION*

W. BUCHMÜLLER and T. HELBIG
Deutsches Elektronen-Synchrotron DESY, Hamburg, Germany

We discuss several aspects of the electroweak phase transition, which is generally believed to be first order. Starting from Langer's theory of metastable states we derive an approximate formula for the decay rate. We then investigate the uncertainties in present evaluations of size and surface tension of critical bubbles and comment on the stumbling blocks on the way towards a quantitative description of the electroweak phase transition.

1. Introduction

Spontaneously broken symmetries are restored at high temperatures.[1-3] The corresponding phase transition associated with the gauge symmetry of weak and electromagnetic interactions (cf. ref. 4) has recently attracted much attention since baryon- and lepton-number violating processes fall out of thermal equilibrium at this transition.[5] Hence, the electroweak phase transition is of crucial importance for our understanding of baryon- and lepton-number asymmetries of the universe and, conversely, these asymmetries can provide valuable information about the evolution of the very early universe.

The electroweak phase transition is generally believed to be first order, and the detailed description of its course, i.e., formation and growth of bubbles or droplets, is a rather involved problem. The usual picture is based on the temperature dependent effective potential $V(\phi, T)$, which is shown in Fig. 1 as function of the order parameter ϕ for different temperatures $T > T' > T_c > T'' > T_b$: at large temperatures V has only a single minimum at $\phi = 0$; as the temperature decreases a second local minimum appears at $\bar{\phi}(T) \neq 0$, which at the critical temperature $T = T_c$ is degenerate with the minimum at $\phi = 0$; for temperatures $T'' < T_c$ the symmetric state with $\phi = 0$ becomes metastable and the height of the potential barrier between $\phi = 0$ and $\bar{\phi} \neq 0$ determines the degree of metastability; finally, at the "barrier temperature" $T_b < T_c$ the potential barrier disappears and the symmetric state becomes unstable.

The process of bubble formation is complicated, it involves quantum tunneling

*Talk given at the XV International Warsaw Meeting on Elementary Particle Physics, Kazimierz, Poland, and HLRZ Workshop on Dynamics of First Order Phase Transitions, Jülich, Germany

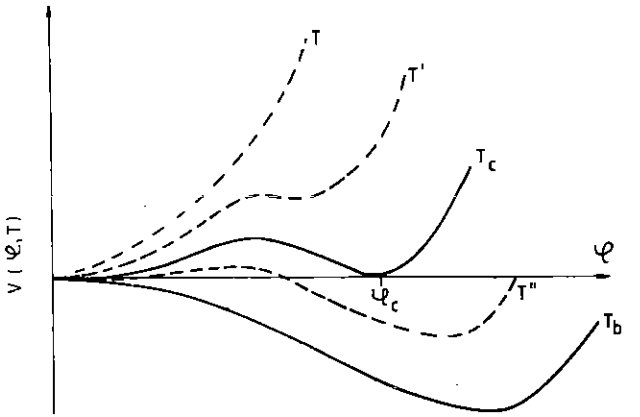

Fig. 1. The effective potential as function of the Higgs field for different temperatures.

as well as thermodynamic fluctuations, which are dominant at high temperatures, and so far a complete treatment of both aspects in quantum field theory is still lacking. In this paper we shall follow Langer's theory for the decay of metastable states,[6] which describes the thermally activated nucleation of bubbles. In sect. 2 a simplified version of this theory will be described, and an approximate formula for the decay rate will be given in the "thin wall approximation".

The decay rate of metastable states is crucially dependent on the effective potential of the system under consideration, which, in the thin wall approximation, reduces to a dependence on surface tension and radius of critical bubbles. The evaluation of the finite temperature effective potential is difficult due to infrared divergencies, and several aspects of this problem have recently been discussed in the literature. In sect. 3 we shall address this problem, for simplicity not for the full electroweak theory but rather for the abelian Higgs model. Finally, in sect. 4 we will compute the temperature T_e, in the range between critical temperature T_c and barrier temperature T_b, where the phase transition is completed. This will then lead us to a discussion of the prospects of obtaining a quantitative description of the electroweak phase transition.

2. Decay of Metastable States

At temperatures below the critical temperature small domains of the energetically favoured, spontaneously broken phase can appear as thermal fluctuations in

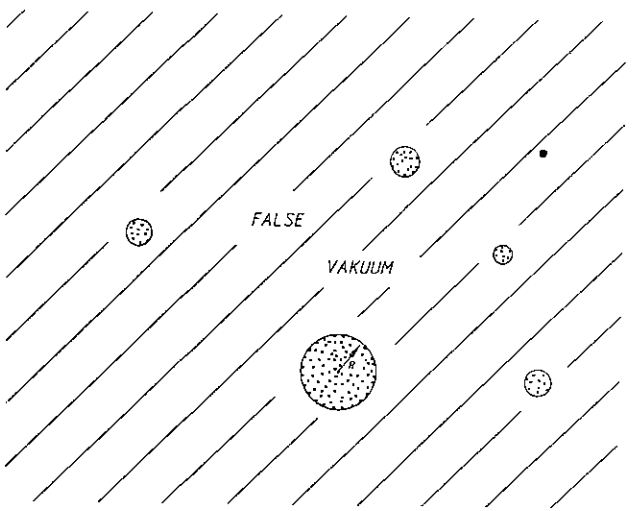

Fig. 2. Some droplets of "true vacuum" embedded in "false vacuum".

the homogeneous, symmetric phase, the so-called "false vacuum". The work needed to form such droplets is, in the thin wall approximation, given by the sum of a positive surface term and a negative volume term:

$$F(R) = 4\pi R^2\sigma - \frac{4\pi}{3}R^3\epsilon. \tag{2.1}$$

Here R, σ and ϵ are droplet radius, surface tension and volume energy density, respectively. $F(R)$ increases at small values of R and decreases at large values of R. At the critical radius R_c it reaches a saddle point:

$$\left.\frac{\partial F}{\partial R}\right|_{R=R_c} = 0, \quad \left.\frac{\partial^2 F}{\partial R^2}\right|_{R=R_c} < 0, \tag{2.2}$$

where $R_c = \frac{2\sigma}{\epsilon}$ and

$$F(R) = \frac{4\pi}{3}R_c^2\sigma - 4\pi(R-R_c)^2\sigma + ... \tag{2.3}$$

Once produced, subcritical droplets ($R < R_c$) shrink, whereas supercritical droplets ($R > R_c$) grow.

For a metastable state it appears reasonable to assume that the multiplicities of small, subcritical droplets per unit volume are given by the Boltzmann distribution[7]:

$$f_0(R) = Ce^{-\beta F(R)}, \ \beta = \frac{1}{T}, \ R \ll R_c, \tag{2.4}$$

where C is an unknown constant. The probability distribution for droplets of arbitrary size is time-dependent and obeys the Fokker-Planck equation[7]:

$$\frac{\partial}{\partial t}f(t,R) + \frac{\partial}{\partial R}s(t,R) = 0, \tag{2.5}$$

where

$$s = Af - B\frac{\partial f}{\partial R}. \tag{2.6}$$

These equations are applicable to droplets much larger than the correlation length. s is a probability current density in "radii space", and the coefficients A and B are related by the requirement that for $s = 0$ the equilibrium distribution (2.4) is a solution of the Fokker-Planck eq. (2.5), i.e.,

$$B = -A\left(\beta\frac{\partial}{\partial R}F\right)^{-1} \tag{2.7}$$

From eqs. (2.1) and (2.6) it is clear that, for large values of R, A is the velocity of the droplet surface.

The continuous process of the phase transition is now described by a stationary solution of the Fokker-Planck equation, i.e., $s = \text{const}$. This constant value of the current density gives the probability per unit time and volume for the nucleation of critical droplets. One obtains (cf. eqs. (2.4), (2.6))[7]:

$$\frac{\Gamma}{V} = s = s(t,R_c) = 2\sqrt{\beta\sigma}BCe^{-\frac{4\pi}{3}\beta\sigma R_c^2}. \tag{2.8}$$

Langer has extended this picture of bubble nucleation to arbitrary fluctuations and he has also determined the constant BC in eq. (2.8). This result for the nucleation probability of critical droplets reads[6]:

$$\frac{\Gamma}{V} = \frac{\kappa}{\sqrt{|\lambda_-|}}\frac{1}{2\pi}\left(\frac{\beta F(\hat{\phi},T)}{2\pi}\right)^{\frac{3}{2}}\left(\frac{\det{}^{>}(F''(\hat{\phi},T))}{\det(F''(0,T))}\right)^{-\frac{1}{2}}e^{-\beta F(\hat{\phi},T)} \tag{2.9}$$

Here $F(\phi,T)$ is the free energy of the system, ϕ is the order parameter, and $\hat{\phi}$ is the saddle point of F which interpolates between the two local minima (cf. Fig. 1); $\det{}^{>}F''$ denotes the product of all positive eigenvalues of F'' at the saddle point, λ_- is the negative eigenvalue; three zero modes due to translational invariance give rise to the pre-factor $F^{\frac{3}{2}}$ and κ is a "dynamical factor" which has recently been related to plasma viscosities by Csernai and Kapusta.[8]

The evaluation of the fluctuation determinant in eq. (2.9) is notoriously difficult. However, in the thin wall approximation one may rather easily sum at least the "Goldstone modes", i.e., those eigenvalues of F'' which vanish if the critical radius R_c goes to infinity (cf. ref. 9). We find the result

$$\frac{\Gamma(T)}{V} \approx \frac{\kappa}{\pi}\left(\frac{1}{3}\beta\sigma\right)^{\frac{3}{2}}(R_c\mu)^{\frac{7}{3}}e^{-\frac{4\pi}{3}\beta\sigma R_c^2}, \tag{2.10}$$

where

$$F(\phi,T) = \int d^3x\left(\frac{1}{2}(\vec{\nabla}\phi)^2 + V(\phi,T)\right), \tag{2.11}$$

$$\sigma = \int_0^{\phi_c} d\phi\sqrt{2V(\phi,T_c)}, \tag{2.12}$$

$$R_c(T) = \frac{2\sigma}{\epsilon},\ \epsilon = V(0,T) - V(\bar{\phi}(T),T), \tag{2.13}$$

$$\mu^2(T) = \left.\frac{\partial^2 V(\phi,T)}{\partial\phi^2}\right|_{\phi=0}. \tag{2.14}$$

$V(\phi,T)$ is the effective potential at finite temperature, $\bar{\phi}(T) \neq 0$ is the local minimum of V at $T \neq 0$ and $\phi_c = \bar{\phi}(T_c)$. Note the non-trivial dependence of the pre-exponential factor in eq. (2.10) on R_c! The formula (2.9) for the nucleation rate of critical bubbles is similar to, but also significantly different from the result obtained by Linde.[10] From eq. (2.10) it is clear that the usual replacement of the entire pre-factor by T^4 is a rather rough approximation. The quantitative effect of the pre-factor on the nucleation rate will be discussed elsewhere.

3. Evaluating the effective potential

The nucleation rate eq. (2.10) depends on surface tension and radius of the critical bubble. In order to compute these quantities, knowledge of the finite temperature effective potential is needed. Based on the one-loop effective potential, a quantitative description of the phase transition has recently been given (cf. Ref. 11 and 12). However, at present the range of validity of the one-loop calculation is very uncertain due to various problems,[13-18] which are related to the infrared properties of perturbation theory in field theories at finite temperature. In the following we will address some of these problems. For simplicity, we will not discuss the full standard model, but restrict ourselves to the simpler case of a $U(1)$ gauge theory.

The corresponding lagrangian of the abelian Higgs model reads

$$L = -\frac{1}{4}F_{\mu\nu}F^{\mu\nu} + (\partial_\mu + ieA_\mu)\Phi^*(\partial^\mu - ieA^\mu)\Phi - V_0(\Phi^*\Phi), \tag{3.1}$$

where the complex scalar field $\Phi = \frac{1}{\sqrt{2}}(\phi + i\chi)$ contains Higgs and Goldstone boson fields ϕ and χ, respectively, A_μ is the vector field with field strength $F_{\mu\nu}$, e is the

gauge coupling constant and V_0 is the scalar potential. In Landau gauge the one-loop finite-temperature correction to the tree-level scalar potential reads (cf. Fig. 3a)

$$V_1(\phi,T) = -\frac{2\pi^2}{45}T^4 + \frac{1}{8}m^2T^2 - \frac{1}{4\pi}m^3T + \frac{3}{64\pi^2}m^4\ln\frac{T}{M} + ..., \tag{3.2}$$

where $m = e\phi$, and M is the renormalisation scale.[3] Due to the term cubic in m the potential has a barrier between the symmetric minimum at $\phi = 0$ and the minimum of the broken phase at $\phi = \bar{\phi}(T) \neq 0$. In eq. (3.2) we have neglected scalar loops, i.e., we restrict ourselves to the case of small Higgs self couplings, $\lambda \ll e^2$. Hence, the potential V_1 does not depend on the masses m_ϕ and m_χ of Higgs boson and Goldstone boson.

At the two-loop level a new term appears in the high temperature expansion of the effective potential which is linear in the vector boson mass m! The two graphs shown in Fig. 3b yield together

$$V_2(\phi,T) = -\frac{e^2}{24\pi}mT^3 + ... \tag{3.3}$$

Such a term would qualitatively change the physical picture derived from the one-loop effective potential. However, the two-loop linear term is cancelled by higher order corrections from "ring-diagrams" (cf. Fig. 3c). The contribution of these diagrams (cf. Ref. 4, 19 and 20) depends on the vacuum polarisation tensor at zero momentum. Since we neglect scalar loops, this corresponds to the longitudinal and transverse "plasma masses" which appear in the photon propagator (cf. Ref. 4),

$$D_{\mu\nu}(k) = \frac{1}{k^2 - \mu_L^2}P_{L\mu\nu} + \frac{1}{k^2 - \mu_T^2}P_{T\mu\nu} + ..., \tag{3.4}$$

where P_L and P_T are the projection operators for longitudinal and transverse polarisation states. For the one-loop finite-temperature corrections to μ_L and μ_T we obtain

$$\delta\mu_L^2 = \frac{e^2}{3}T^2 - \frac{e^2}{\pi}mT + ..., \tag{3.5}$$

$$\delta\mu_T^2 = -\frac{2e^2}{3\pi}mT + ... \tag{3.6}$$

Note that for values of the Higgs field smaller than

$$\phi_1 = \frac{2e}{3\pi}T \tag{3.7}$$

$\mu_T^2 = m^2 + \delta\mu_L^2$ becomes negativ, and the perturbation expansion breaks down.

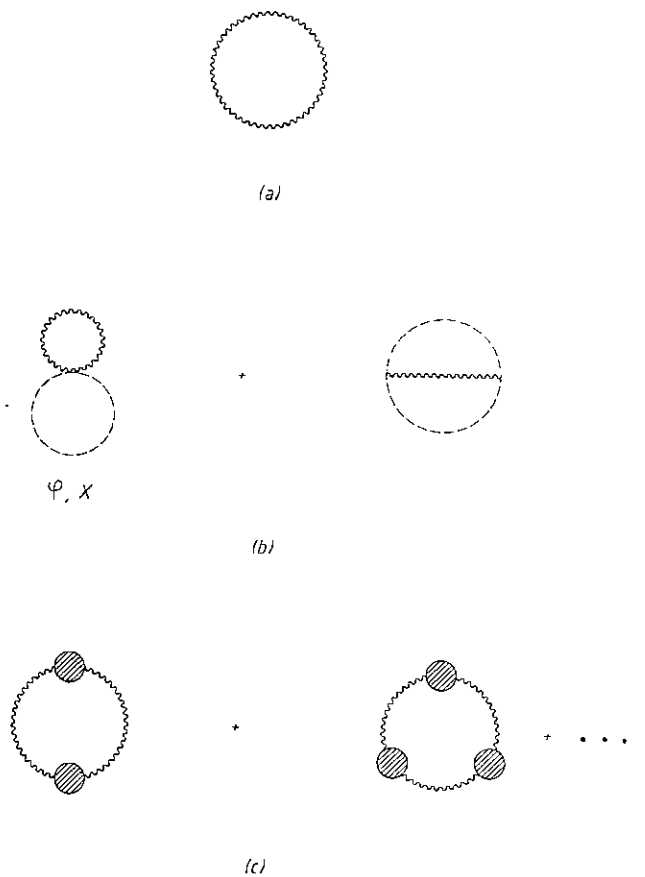

Fig. 3. Contributions to the effective potential: (a) one-loop, (b) two-loop, (c) ring diagrams.

The contribution of the ring diagrams to the effective potential is easily evaluated. One obtains

$$\begin{aligned} V_1 + V_{RING} = &-\frac{2\pi^2}{45}T^4 + \frac{1}{8}m^2T^2 \\ &- \frac{1}{12\pi}\left[(m^2+\delta\mu_L^2)^{\frac{3}{2}} + 2(m^2+\delta\mu_T^2)^{\frac{3}{2}} - \frac{3}{2}m(\delta\mu_L^2+\delta\mu_T^2)\right]T \\ &+ \frac{1}{64\pi^2}\left[(m^2+\delta\mu_L^2)^{\frac{3}{2}} + (m^2+\delta\mu_T^2)^{\frac{3}{2}}\right. \\ &\left. - 2m^2(\delta\mu_L^2+2\delta\mu_T^2)\right]\ln\frac{T^2}{M^2}. \end{aligned} \tag{3.8}$$

Using eq. (3.5) one easily verifies that the term in eq. (3.8) proportional to $m\delta\mu_L^2 T \sim e^2 mT^3$ precisely cancels the two-loop term linear in m (cf. eq. (3.3)). As expected, there remains a linear Term $\sim e^3 mT^3$ since also three-loop graphs, which have not been taken into account, contribute at the same order in e.

The remaining dominant effect of the ring diagrams is due to the longitudinal mass $\delta\mu_L^2$. For small values of m this effectively reduces the strength of the cubic term in $V_1 \sim m^3T$ by $\frac{1}{3}$, as already pointed out by Dine et al.[17] In Fig. 5 the effective potential is shown for $\phi > \phi_1$ (cf. eq. (3.7)) for three cases: one-loop (A), ring improvement with $\delta\mu_L^2 = \frac{e^2}{3}T^2$, $\delta\mu_T^2 = 0$ (B) and ring improvement with $\delta\mu_L^2$, $\delta\mu_T^2$ according to eqs. (3.5), (3.6). The three potentials are plotted for the corresponding three critical temperatures $T_c = 150$ GeV (A), $T_c = 154$ GeV (B) and $T_c = 142$ GeV (C) which we have obtained after extrapolating the three potentials smoothly to $\phi = 0$. We have chosen $e = g$, where g is the Standard Model SU(2) gauge coupling, and the Higgs field at zero temperature is $\phi_0 = 246$ GeV. The difference between the three potentials illustrates the uncertainty due to unknown higher order corrections.

An important question is the behaviour of the magnetic mass μ_T as m approaches 0. This requires to go beyond the one-loop approximation. As a first step we have solved the one-loop gap equation (cf. Fig. 4) at zero momentum. In Landau gauge we find the following result in the high temperature expansion up to terms of order $\ln T$ (Ref. 21):

$$\begin{aligned} \delta\mu_L^2 = &\frac{e^2}{3}T^2 - \frac{e^2}{4\pi}\left(4\frac{m^2}{\mu_L+m_\phi} + m_\phi + m_\chi\right)T \\ &- \frac{3e^2}{16\pi^2}\frac{m^2}{\mu_L^2-m_\phi^2}\left(\mu_L^2\ln\frac{\mu_L^2}{T^2} - m_\phi^2\ln\frac{m_\phi^2}{T^2}\right), \end{aligned} \tag{3.9}$$

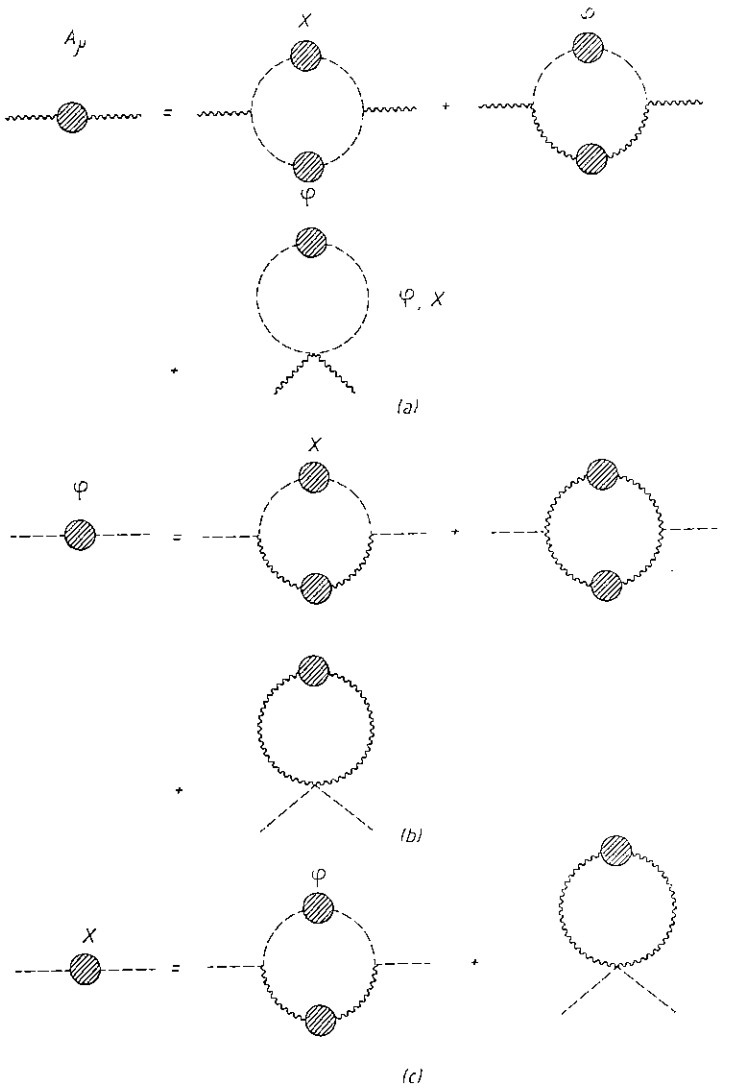

Fig. 4. One-loop gap equations for vector (A_μ) and scalar (ϕ, χ) propagators.

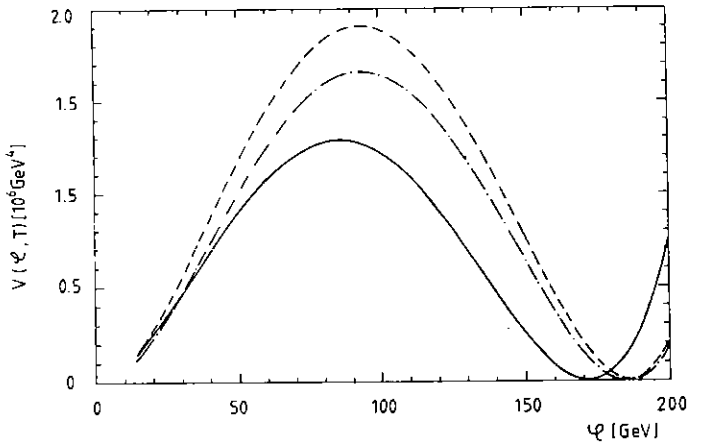

Fig. 5. Three effective potentials at their respective critical temperatures (see text): (A) one-loop (dashed), (B) ring improvement without "linear terms" (dash-dotted), (C) ring improvement with "linear terms" (full). All potentials are plotted for $\phi > \phi_1$, where the one-loop approximation breaks down.

$$\delta\mu_T^2 = \frac{e^2}{12\pi}\left(-8\frac{m^2}{\mu_T+m_\phi}+\frac{(m_\phi-m_\chi)^2}{m_\phi+m_\chi}\right)T - \frac{e^2}{48\pi^2}\frac{m^2}{\mu_L^2-m_\phi^2}\left(\mu_L^2\ln\frac{\mu_L^2}{T^2}-m_\phi^2\ln\frac{m_\phi^2}{T^2}\right) - \frac{e^2}{6\pi^2}\frac{m^2}{\mu_T^2-m_\phi^2}\left(\mu_T^2\ln\frac{\mu_T^2}{T^2}-m_\phi^2\ln\frac{m_\phi^2}{T^2}\right), \tag{3.10}$$

$$\delta m_\phi^2 = \frac{e^2}{4}T^2 - \frac{e^2}{4\pi}\left(\mu_L+2\mu_T+\frac{m^2}{\mu_L}+2\frac{m^2}{\mu_T}\right)T - \frac{e^2}{16\pi^2}\left((\mu_L^2+2m^2)\ln\frac{\mu_L^2}{T^2}+2(\mu_T^2+2m^2)\ln\frac{\mu_T^2}{T^2}\right), \tag{3.11}$$

$$\delta m_\chi^2 = \frac{e^2}{4}T^2 - \frac{e^2}{4\pi}(\mu_L+2\mu_T)T - \frac{e^2}{16\pi^2}\left(\mu_L^2\ln\frac{\mu_L^2}{T^2}+2\mu_T^2\ln\frac{\mu_T^2}{T^2}\right). \tag{3.12}$$

Since m_ϕ gets a plasma mass $\sim e^2T^2$ one obtains for $m \to 0$, as expected,

$$\mu_T \sim m\left(1-\frac{e^2}{3\pi}+\ldots\right), \tag{3.13}$$

i.e., at $\phi = 0$ the transverse photon mass vanishes. Since all mass terms now remain positive for $m \to 0$, this result suggests that it may be possible to compute the effective potential also at small values of ϕ by using improved propagators.

4. The Phase Transition

Given the free energy, as discussed in the previous sect., we are now able to evaluate critical radius, surface tension and correlation length. For the three potentials of Fig. 5 we find for T_c, R_c^{-1}, σ and μ: (150 GeV, 7.1 GeV, $2.4 \cdot 10^5$ GeV^3, 27 GeV) (A), (154 GeV, 6.7 GeV, $2.2 \cdot 10^5$ GeV^3, 29 GeV) (B), (142 GeV, 6.4 GeV, $1.9 \cdot 10^5$ GeV^3, 23 GeV) (C). Using eq. (2.10) and choosing $\kappa = T$ one easily obtaines the nucleation rates per unit time and volume for the three cases.

At what temperature is the phase transition completed? Following ref. 22 one obtains for the corresponding time t_e:

$$\int_{t_c}^{t_e} dt' \Gamma(t') a^3(t_e) \frac{4\pi}{3} \left(\int_{t'}^{t_e} dt'' \frac{v(t'')}{a(t'')} \right)^3 \left(\ln f(t_e)^{-1} \right)^{-1} = 1. \qquad (4.1)$$

Here $a(t)$ is the FRW scale factor, $v(t)$ is the velocity of the droplet surface, and time and temperature are related by $t = 0.03 \frac{m_{PL}}{T^2}$, where m_{PL} is the Planck mass. $f(t_e)$ is the fraction of space left over in false vacuum at time t_e. From eq. (4.1) one derives a condition for a rough estimate of t_e:

$$\Gamma(t_e) t_e^4 \sim 1. \qquad (4.2)$$

Using this condition we find for the temperatures T_e at which the phase transition is completed $T_e = 145$ GeV (A), 149 GeV (B), 139 GeV (C). The temperature T_b, at which the potential wall disappears, is given by $T_b = \frac{2\sqrt{\lambda}}{e} \phi_0 \approx 115$ GeV for $\lambda \approx 0.1 e^2$. Comparing the temperatures T_c, T_e and T_b it is clear that, for sufficiently small Higgs boson masses, the phase transition is completed at a temperature T_e satisfying

$$\frac{T_c - T_e}{T_c - T_b} \ll 1. \qquad (4.3)$$

For large Higgs masses this condition is not satisfied and the scalar plasma masses can no longer be considered heavy, i.e., $\sim e^2 T^2$.

So far, we have only considered the abelian Higgs model with small scalar couplings, i.e., $\lambda \ll e^2$. What can we learn from this discussion for the electroweak phase transition which is of physical interest? First of all, for small Higgs boson and fermion masses it appears possible to evaluate the free energy sufficiently accurate by means of an improved perturbation theory which takes plasma masses into account, although a systematic expansion at all values of ϕ, such that errors are under control, is still lacking. For large values of scalar self couplings and Yukawa couplings $T_c - T_b$ and $T_e - T_b$ decrease, the loop expansion becomes less convergent and eventually breaks down - the first order transition approaches a second order

one. Furthermore, for the nonabelian SU(2) gauge interaction, the nonperturbative problem of the magnetic mass of the W-Boson has to be addressed. Given the free energy of the Standard Model the picture of bubble nucleation has to be carefully examined. This includes corrections to the nucleation rate, the validity of the thin wall approximation, computation of the bubble surface velocity, the coalescence of bubbles etc. To conclude, the quantitative description of the electroweak phase transition is certainly a challenging problem, however, given the methods available in quantum field theory and condensed matter physics, it appears within reach.

References

1. D. A. Kirzhnits and A. D. Linde, *Phys. Lett.* **B72** (1972) 471.
2. S. Weinberg, *Phys. Rev.* **D9** (1974) 3357.
3. L. Dolan and R. Jackiw, *Phys. Rev.* **D9** (1974) 3320.
4. J. I. Kapusta, *Finite Temperature Field Theory*, (Cambridge Univ. Press, 1989).
5. For a recent review, see E. Kolb, these proceedings;
   M. E. Shaposhnikov, "Anomalous Fermion Number Non-conservation", preprint CERN-TH 6304/91 (1991).
6. J. Langer, *Ann. Phys.* **54** (1969) 258.
7. E. M. Lifshitz and L. P. Pitaevskii, *Physical Kinetics*, (Pergamon, 1980) part 1.
8. L. P. Csernai and J. I. Kapusta, preprint TPI-MINN-92/10-T (1992).
9. N. J. Günther, D. A. Nicole and D. J. Wallace, *J. Phys A: Math. Gen.* **13** (1980) 1755.
10. A. D. Linde, *Nucl. Phys.* **B216** (1983) 421.
11. K. Enqvist, J. Ignatius, K. Kajantie and K. Rummukainen, *Phys. Rev.* **D45** (1992) 3415.
12. G. W. Anderson, preprint UCB-PTH-91/46 (1991).
13. D. E. Brahm and S. D. H. Hsu, preprint CALT-68-1705 (1991);
    C. G. Boyd, D. E. Brahm and S. D. H. Hsu, preprint CALT-68-1795 (1992).
14. M. E. Shaposhnikov, *Phys. Lett.* **B277** (1992) 324; preprint CERN-TH 6319/91 (1992).
15. N. Tetradis, preprint DESY 91-151 (1991).
16. M. Gleiser and E. Kolb, preprint FERMILAB-Pub-91/305-A (1991)
17. M. Dine *et al.*, *Phys. Rev.* **D46** (1992) 550.
18. N. Tetradis and C. Wetterich, preprint DESY 92-093 (1992).
19. K. Takahashi, *Z. Phys.* **C26** (1985) 601.
20. M. E. Carrington, *Phys. Rev.* **D45** (1992) 2933.
21. W. Buchmüller, T. Helbig and D. Walliser, in preparation.
22. A. Guth and E. Weinberg, *Phys. Rev.* **D23** (1981) 876.